Niche partitioning facilitates coexistence of closely related gut bacteria

Silvia Brochet[a], Andrew Quinn[a], Ruben A.T. Mars[b], Nicolas Neuschwander[a], Uwe Sauer[b], Philipp Engel[a]

[a]Department of Fundamental Microbiology, University of Lausanne, 1015 Lausanne, Switzerland

[b]Institute of Molecular Systems Biology, ETH Zürich, Zürich, Switzerland

Correspondence:

Prof. Philipp Engel

Department of Fundamental Microbiology

University of Lausanne, CH-1015 Lausanne, Switzerland

Tel.: +41 (0)21 692 56 12

e-mail: philipp.engel@unil.ch

Abstract

Ecological processes underlying bacterial coexistence in the gut are not well understood. Here, we disentangled the effect of the host and the diet on the coexistence of four closely related *Lactobacillus* species colonizing the honey bee gut. We serially passaged the four species through gnotobiotic bees and in liquid cultures in the presence of either pollen (bee diet) or simple sugars. Although the four species engaged in negative interactions, they were able to stably coexist, both *in vivo* and *in vitro*. However, coexistence was only possible in the presence of pollen, and not in simple sugars, independent of the environment. Using metatranscriptomics and metabolomics, we found that the four species utilize different pollen-derived carbohydrate substrates indicating resource partitioning as the basis of coexistence. Our results show that despite longstanding host association, gut bacterial interactions can be recapitulated *in vitro* providing insights about bacterial coexistence when combined with *in vivo* experiments.

38 **Introduction**

39

40 Gut microbial communities are usually dominated by few bacterial phyla and
41 families, but contain a high extent of species- and strain-level diversity[1,2]. According to
42 the competition-relatedness hypothesis, the more closely two organisms are related the
43 more likely it is that they will compete and exclude each other due to overlapping niches[3].
44 Therefore, it has remained unclear how closely related microbes can be maintained in the
45 gut, or in any other natural microbial ecosystem.

46 The high concentration of nutrients and the structured environment of the gut
47 may allow functionally redundant species or strains to coexist[4]. The host may even select
48 for such redundancy, as it can increase the stability and resilience of the microbiota
49 against environmental disturbance[4,5]. Phage predation can also contribute to the
50 maintenance of diversity by imposing kill-the-winner dynamics and hindering the
51 outgrowth of a single dominant strain[6]. Another possibility is that closely related species,
52 and even strains of the same species, have functionally diverged from each other and
53 occupy distinct ecological niches[7,8]. The genomic flexibility of bacteria facilitates
54 adaptation to different nutrients, provided in the diet or by the host[9,10], or result from
55 interactions with other bacteria[11], such as cross-feeding[12] or cooperative glycan
56 breakdown[13].

57 Few experimental studies have investigated the coexistence of bacteria in host-
58 associated microbial communities. The high diversity in these ecosystems and the
59 resistance of many host-associated bacteria to experimental manipulations introduce
60 considerable challenges for such approaches[14,15]. Moreover, community dynamics
61 observed *in vivo* can be difficult to reproduce under laboratory conditions, as the host
62 presents a highly specialized nutritional and spatial environment. Thus, there is a need

63 for *in vitro* models that can reproduce ecological interactions observed *in vivo*, from
64 simple co-culturing setups[16] to sophisticated 'organoids-on-a-chip' systems [17,18].
65 The gut microbiota of the Western honey bee (*Apis mellifera*) is composed of a few
66 deep-branching phylogenetic lineages (phylotypes) belonging to the Firmicutes,
67 Actinobacteria and Proteobacteria phyla[19,20]. Most of these lineages are composed of
68 several closely related sequence-discrete populations, hereafter referred to as species,
69 each of which contains further diversity at the strain-level[21–24]. Microbiota-depleted bees
70 can be generated and experimentally colonized with synthetic communities of different
71 strains. Moreover, most community members can be cultured in pollen, which is the
72 major dietary source of honey bees[25]. This experimental tractability offers an excellent
73 opportunity to probe the coexistence of bacteria in the gut of their native host and in
74 controlled laboratory cultures using similar nutritional conditions.
75 One of the most abundant and diverse phylotype of the honey bee gut microbiota
76 is *Lactobacillus* Firm5[22]. This phylotype consists of facultative anaerobes that ferment
77 sugars into organic acids and utilize various pollen-derived glycosylated plant
78 compounds, such as flavonoids[25]. *Lactobacillus* Firm5 is specific to social bees but has
79 diverged into many different species of which four are specifically associated with the
80 Western honey bee, *Apis mellifera*: *Lactobacillus apis* (Lapi), *Lactobacillus*
81 *helsingborgensis* (Lhel), *Lactobacillus melliventris* (Lmel) and *Lactobacillus kullabergensis*
82 (Lkul). The four species are consistently present in the gut of individual honey bees
83 suggesting that they can share the available niches and stably coexist despite their
84 phylogenetic relatedness. Genomic analysis has revealed that these species share <85%
85 pairwise average nucleotide identities (gANI) and exhibit high levels of genomic variation
86 in terms of carbohydrate metabolism[22,24]. However, whether the coexistence is facilitated
87 by adaptation to different nutritional niches, and to what extent the host environment,

88 the diet, or the interactions with other community members matter is currently
89 unknown.

90 Here, we tested under which conditions the four *Lactobacillus* Firm5 species can
91 coexist and investigated the underlying molecular mechanism. We serially passaged the
92 four species *in vivo* through gnotobiotic bees and *in vitro* in liquid cultures, and applied
93 RNA sequencing and metabolomics analysis. Our results show that the coexistence of the
94 four species is mediated by the partitioning of nutrients derived from the pollen diet of
95 bees and is largely independent from the presence of the host or other community
96 members.

97

98 ## Results

99

100 **The coexistence of four related *Lactobacillus* species in the honey bee gut depends**
101 **on the host diet**

102 All experiments in this study were conducted with four bacterial isolates
103 representing the four *Lactobacillus* Firm5 species (Lapi, Lhel, Lmel, and Lkul) associated
104 with the Western honey bee. We first tested if the four species can establish in the gut of
105 gnotobiotic bees under two different dietary conditions. To this end, we colonized
106 microbiota-depleted bees with each of the four species, alone or together, and fed bees
107 either sterilized sugar water (SW) or sterilized sugar water and pollen (SW+PG). Five
108 days post-colonization we assessed the bacterial loads in the gut by counting CFUs
109 (**Figure 1A, Supplementary Dataset 1**). When mono-colonized, the four species
110 established in the gut of microbiota-depleted bees independent of the dietary treatment
111 (**Figure 1A**). In the SW treatment, the colonization levels were generally lower than in
112 the SW+PG treatment (**Figure 1A**, ANOVA q-value < 0.01) confirming previous results
113 that pollen increases the total bacterial load in the gut[26]. There was no statistically
114 significant difference between the total bacterial loads of the mono-colonizations and the
115 co-colonizations in either dietary treatment, with the exception of the mono-colonization
116 with Lkul, which showed higher loads than the co-colonizations in SW (**Figure 1A**,
117 ANOVA q-value < 0.01). Consequently, the sum of the bacterial loads of the mono-
118 colonizations exceeded the total bacterial load of the co-colonizations in both dietary
119 treatments, suggesting that the species engage in negative interactions when colonizing
120 the honey bee gut together.

121 To test if the four species can stably coexist in the bee gut, we serially passaged
122 the community seven times in microbiota-depleted bees under both dietary conditions

123 (SW and SW+PG). After each passage (i.e. after 5 days of colonization), we used amplicon
124 sequencing of a discriminatory housekeeping gene fragment (see Materials and methods)
125 in combination with CFU counting to determine the absolute abundance of each species
126 in the community. We observed clear differences between the two dietary conditions in
127 the ability of the four species to coexist across the passages (**Figure 1B-C,**
128 **Supplementary Dataset 2**). In the SW treatment, all species were initially detectable in
129 most samples (P1, **Figure 1B**). However, three species (Lapi, Lmel and Lkul) steadily
130 decreased in abundance in the subsequent passages resulting in a rapid dominance of
131 Lhel (**Figure 1B**). Lmel and Lkul reached the detection limit and Lapi decreased to around
132 10^4 bacteria/gut by passage five (P5, **Figure 1B**). Only Lhel was stably maintained across
133 all seven passages and was present at around 1000x higher abundance than Lapi at the
134 end of the experiment (~10^7 bacteria/gut, **Figure 1B**). In the contrary, in the SW+PG
135 treatment, all four species were detectable in all passages at around 10^6 to 10^8
136 bacteria/gut, and displayed a highly stable abundance profile over time (**Figure 1C**).
137 In summary, these findings show that the four species can stably coexist *in vivo*
138 when bees are fed pollen, but not when they are only fed sugar water. This is consistent
139 with the idea that pollen facilitates niche partitioning in the honey bee gut by offering
140 competing species different ecological niches facilitating their coexistence.
141
142 ***In vitro* co-culture experiments recapitulate the nutrient-dependent coexistence of**
143 **the four *Lactobacillus* species**
144 We next tested if the four species can also coexist *in vitro*, outside of the host
145 environment, under different nutrient conditions. To this end, we cultured the species
146 alone or together in minimal medium supplemented with either glucose (G), pollen
147 extract (PE), or entire pollen grains (PG). All four species were able to grow when

148 cultured alone under the three nutrient conditions (**Supplementary Figure 1,**
149 **Supplementary Dataset 1**). Growth yields of Lhel, Lkul, and the co-culture were slightly
150 lower in PE and PG than in G, and Lmel showed lower growth yields than some of the
151 other species in PE and G (**Supplementary Figure 1,** ANOVA q-value < 0.01). As *in vivo*,
152 the total bacterial loads of the co-cultures were not consistently different from those of
153 the mono-cultures (**Supplementary Figure 1**), suggesting that the four species have
154 overlapping metabolic niches and engage in negative interactions with each other.

155 We then serially passaged the co-cultures 21 times under the three different
156 nutrient conditions by transferring an aliquot after 24 h of growth into fresh culture
157 medium (1:20). The absolute abundance of each strain was determined after every other
158 passage by combining amplicon sequencing with qPCR (see Materials and methods). As
159 for the *in vivo* experiment, we observed clear differences in the growth dynamics of the
160 four species, both over time and between the glucose and the pollen culture conditions
161 (**Figure 2, Supplementary Dataset 2**). In the presence of glucose, three of the four
162 species (Lhel, Lmel and Lkul) steadily decreased in abundance over time (**Figure 2A**),
163 with two of them reaching the limit of detection ($<10^5$ bacteria/ml) after about 11
164 passages (P11). In contrast, Lapi was stably maintained at high abundance (10^9
165 bacteria/ml) until the last passage (**Figure 2A**) and hence dominated the co-culture for
166 most of the transfer experiment. In the presence of PE or PG, the four species revealed
167 very different growth behaviors (**Figure 2B and 2C**). None of the species decreased over
168 time, and after 21 transfers all species still yielded between 10^6-10^9 bacteria/ml.

169 To look at changes in community composition over time, we measured the
170 community stability (temporal mean divided by temporal standard deviation of the
171 species abundances) in sliding windows of five passages. Little to no change in
172 community stability was observed for the two pollen conditions throughout the

173 experiment, whereas in glucose the community reached a stable state after ~11 transfers
174 (**Figure 2D**). To compare the growth yields of each species across the three nutrient
175 conditions, we only considered the passages after which community stability was
176 reached (P13-21). With the exception of Lapi all species reached higher yields in the
177 presence of pollen as compared to glucose (**Figure 2E**, ANOVA q-value < 0.01). Notably,
178 Lmel was the only species that showed improved growth in PG as compared to PE (**Figure**
179 **2A-C**).

180 In summary, these findings show that the nutrient-dependent coexistence of the
181 four *Lactobacillus* species observed *in vivo* can be recapitulated *in vitro* in a simple co-
182 culture experiment, suggesting that the partitioning of pollen-derived nutrients is
183 sufficient for enabling coexistence. Similar results were obtained for a second *in vitro*
184 experiment which included the same nutrient conditions, but was only conducted for ten
185 transfers (**Supplementary Figure 2**).

186

187 **The four *Lactobacillus* species upregulate divergent carbohydrate transport and**
188 **metabolism functions in the presence of pollen during gut colonization**

189 Given the impact of pollen on the coexistence of the four *Lactobacillus* species, we
190 tested if genes involved in nutrient acquisition and metabolism were differentially
191 expressed between the dietary treatments. To this end, we carried out RNA sequencing
192 of the four-species community in honey bees that were fed either sugar water (SW) or
193 sugar water and pollen grains (SW+PG) (**Figure 3A**). Multidimensional scaling (MDS) of
194 the normalized read counts mapped to each species revealed that most samples clustered
195 by treatment (SW+PG versus SW) (**Supplementary Figure 3**), indicating that all four
196 species exhibited dietary-specific transcriptional responses.

197 We found a total 687 genes (181 to 217 genes per species) to be differentially
198 expressed ($\log_2 FC \geq |2|$ and p-value ≤ 0.01) between the two dietary treatments (**Figure**
199 **3B**). "Carbohydrate transport and metabolism" (Cluster of orthologous group category G,
200 COG G) was by far the most abundant functional category among the genes upregulated
201 in the SW+PG treatment relative to the SW treatment (**Figure 3C,** 17.1-37.6% of all
202 upregulated genes). In three of the four species (Lmel, Lhel, and Lkul), this category was
203 significantly enriched among the upregulated genes (Fisher's exact test, $p<0.01$,
204 **Supplementary Dataset 4)**. The largest fraction of the upregulated COG G genes encoded
205 PTS transporters (**Figure 3D, Supplementary Dataset 3)**, followed by other sugar
206 transporters (e.g. ABC transporters), and enzymes involved in sugar cleavage and
207 conversion (**Figure 3D**). Among the downregulated genes, COG G genes were not
208 abundant (5.1-7.8%) (**Figure 3C**). Instead, the category "Amino acid metabolism and
209 transport" (COG E) was enriched in Lapi (Fisher's exact test, $p < 0.01$, **Supplementary**
210 **Dataset 6**), and genes encoding ABC-type amino acid transporters were present among
211 the downregulated genes in all species (**Supplementary Dataset 3)**.
212 We next clustered all genes by homology into gene families. While most of the
213 differentially expressed genes (89%) belonged to gene families with homologs in
214 multiple species, differential expression was typically observed for just one of the species
215 (**Figure 3E-F**). This suggests that the presence of pollen triggers distinct transcriptional
216 changes in the four species during gut colonization. Indeed, gene annotation analysis
217 allowed us to identify several species-specific metabolic functions among the
218 differentially regulated genes (**Figure 4, Supplementary Dataset 3**). For example, Lhel
219 specifically upregulated three PTS gene clusters for the uptake and metabolism of sugar
220 alcohols and one gene cluster for ribose utilization. In contrast, Lmel upregulated several
221 gene clusters involved in the cleavage of xylose, mannose, rhamnose, and arabinose from

222 polysaccharides or other glycosylated compounds. Lmel also upregulated a gene cluster
223 for the synthesis and the transport of bacteriocins in the presence of pollen. Lkul
224 upregulated a starch utilization gene cluster, which in part was also differentially
225 regulated in Lmel. In addition, this species upregulated an oligopeptide transporter gene
226 cluster that was present in some of the other strains but not differentially regulated. The
227 fourth species, Lapi, also differentially expressed genes belonging to COG 'G' (mainly PTS
228 transporters), but fewer ones, and with similar functional annotations as found in the
229 other three species. However, Lapi was the only species that upregulated two conserved
230 deoxycytidine kinase genes encoding enzymes involved in nucleoside salvage pathways.
231 Besides these species-specific transcriptional changes, a number of interesting
232 functions were differentially regulated in more than one species. For example, we found
233 evidence for citrate fermentation in Lhel and Lkul. Both species upregulated genes
234 encoding a citrate lyase for the conversion of citrate into oxaloacetate and acetate in the
235 presence of pollen (**Supplementary Dataset 3)**. Lhel, Lmel, and Lkul upregulated genes
236 for the uptake and metabolism of glycerol. Moreover, all four species upregulated gene
237 clusters encoding surface proteins with leucine-rich repeat (LRR) regions, LPXT cell-wall
238 anchoring motifs, and SLAP (S-layer associated protein) domains (**Figure 3G**).
239 Altogether, these results suggest that the four species utilize different
240 carbohydrate-related resources from pollen, which supports the niche partitioning
241 hypothesis as the basis for coexistence.
242
243 **Transcriptional responses to pollen are similar *in vivo* and *in vitro***
244 *In vivo* gene expression differences between the two dietary conditions could be
245 influenced by the host or by bacteria-bacteria interactions. Therefore, we carried out an
246 additional transcriptomics analysis to disentangle the contribution of each of these

247 factors to transcriptional changes in the four *Lactobacillus* species. We grew the four
248 species *in vitro* in either co-culture or mono-culture, and with either pollen extract (PE)
249 or glucose as growth substrate (G) (**Figure 5A**). As for the *in vivo* RNA-Seq analysis, MDS
250 plots of the normalized read counts indicated that the four species exhibit treatment-
251 specific transcriptional responses (**Supplementary Figure 4**).

252 For each species, whether grown alone or in co-culture, we found between 159-
253 393 genes to be differentially regulated between the PE and the G treatment (**Figure 5B**,
254 $\log_2 FC \geq |2|$ and p-value$\leq$0.01). As *in vivo*, Carbohydrate transport and metabolism (COG
255 'G') was the predominant functional category among the upregulated genes in the
256 presence of pollen (**Figure 5C**) and enriched in all eight comparisons (four species , each
257 alone or in co-culture, Fisher's exact test p-value < 0.01, **Supplementary Dataset 6**).
258 Moreover, 25.3%-36.9% of the genes upregulated *in vivo* were also upregulated *in vitro*
259 in the presence of pollen. In particular, the species-specific carbohydrate metabolism
260 functions described above (**Figure 4**) showed a similar transcriptional response to pollen
261 *in vivo* and *in vitro* (**Figure 5D**). In contrast, most of the putative adhesin genes
262 upregulated *in vivo* were not upregulated *in vitro* during growth in pollen or had
263 relatively low transcripts per million (TPM). This suggests that these genes are either
264 expressed in response to the host environment , or the presence of entire pollen grains
265 or sugar water, both of which were only included in the *in vivo* but not in the *in vitro*
266 experiment (**Supplementary Dataset 7**). It is also noteworthy that fewer genes were
267 downregulated than upregulated in pollen relative to glucose, and that the COG category
268 'G' was not enriched among the downregulated genes, which is concordant with our *in*
269 *vivo* transcriptome analysis. (**Supplementary Dataset 6**). Based on these results, we
270 conclude that each species upregulates specific operons for the transport and utilization

271 of different carbohydrates (e.g. sugar alcohols and glycans) in response to the presence
272 of pollen, independent of the host environment.
273
274 **The presence of other community members has little impact on the transcriptional**
275 **profile of the four species**
276 We found that a large fraction of the genes upregulated in PE relative to G in the
277 mono-cultures were also upregulated in the co-cultures (58.2-87.8%, **Figure 5E**). In
278 particular, the gene clusters identified to be regulated in a species-specific manner (see
279 above) showed highly concordant gene expression profiles *in vitro* independent of the
280 presence/absence of the other *Lactobacillus* species. This was confirmed by the direct
281 comparison of mono-culture and co-culture conditions. In comparison to the nutritional
282 treatments, fewer genes (9-149 genes) were differentially expressed between co-culture
283 and mono-culture treatments ($\log_2 FC \geq |2|$ and p-value$\leq$0.01), (**Figure 5F**).
284 We could not find any consistent pattern across the four species in terms of COG
285 category enrichment (**Supplementary Dataset 6**). Moreover, only a few genes were
286 differentially expressed in more than one species (6.25-30%), or across both nutrient
287 conditions (1.86-5.33%). Citrate fermentation genes were upregulated in Lkul in co-
288 culture relative to mono-culture when grown in pollen, whereas in Lhel the opposite was
289 observed (**Figure 5G**). Also of note, the oligopeptide transporter system which was
290 upregulated *in vivo* in Lkul in the presence of pollen, was also upregulated *in vitro* in the
291 presence of pollen, but only when other species were present. These two specific
292 examples show that a few metabolic functions are differentially regulated in response to
293 other bacteria, but not always in the same direction across species, or only in a specific
294 nutrient condition. We thus conclude that the main factor driving changes in gene

295 expression in the four strains is the presence of pollen, rather than the presence of other
296 *Lactobacillus* species.
297
298 **Metabolomics analysis reveals differences in flavonoid and sugar metabolism**
299 **across the four *Lactobacillus* species**
300 Our transcriptome analyses suggest that differences in sugar metabolism may
301 enable the four species to coexist in the presence of pollen *in vitro* and *in vivo*. To assess
302 species-specific metabolic changes when grown in pollen, we profiled the metabolome of
303 the pollen extract medium before (t = 0h) and after bacterial growth (t = 16h) using Q-
304 TOF-based untargeted metabolomics[27]. We annotated a total of 657 ions of which 406
305 could be reliably categorized as pollen-derived ions, as opposed to ions originating from
306 the base medium (see methods, **Supplementary Dataset 8**, **Supplementary Figure 6**).
307 The metabolomics data clearly separated the four species indicating distinctive metabolic
308 changes and thus corroborating the transcriptome results (**Supplementary Figure 5**). A
309 total of 76 pollen-derived ions showed a significant decrease in abundance over-time
310 (log2FC ≤ -1 and p-value≤0.01, Student's t-Test, BH correction) (**Figure 6A,**
311 **Supplementary Dataset 8**). Of those, 24 ions decreased in abundance in all four species,
312 another 24 ions decreased in abundance in only a subset of the species, and the remaining
313 28 ions decreased in abundance in only a single species (**Figure 6A**). Ions annotated as
314 glycosylated flavonoids were among the top ions responsible for the separation of the
315 four species in the PCA (**Supplementary Figure 5**). Lmel depleted six different ions
316 annotated as flavonoids (isoorientin 2''-O-rhamnoside, quercetin-3-O-glucoside, vitexin,
317 rutin, luteolin-7-O-(6''-malonylglucoside), and quercetin-3-O-beta-D-glucosyl-(1->2)-
318 beta-D-glucoside), while Lapi depleted three ions annotated as flavonoids (isoorientin
319 2''-O-rhamnoside, quercetin-3-O-glucoside, vitexin) (**Figure 6A, Supplementary Figure**

320 **7**). In contrast, Lkul only depleted the flavonoid ion annotated as isoorientin 2''-O-
321 rhamnoside, and no flavonoid ion changes were identified for Lhel (**Figure 6A,**
322 **Supplementary Figure 7**).

323 To corroborate the species-specific utilization of flavonoids, we incubated each of
324 the four species in base culture medium supplemented with rutin. We observed the
325 formation of a yellow insoluble precipitate only in the wells incubated with Lmel (**Figure**
326 **6B**). Metabolomics analysis confirmed that rutin was depleted in these wells and that the
327 yellow precipitate corresponded to an accumulation of quercetin, the water-insoluble,
328 deglycosylated aglycone of rutin (**Figure 6C**). These findings are consistent with our
329 transcriptome results which show that Lmel is the only species that upregulated a
330 rhamnosidase gene known to cleave rhamnose residue from rutin[28] (**Figure 4**).

331 Other ions with species-specific abundance changes included a plant-derived
332 glycosylated compound belonging to the iridioids class (i.e. antirrhinoside, depleted in
333 the presence of Lapi), a component of the outer pollen wall (i.e. 9,10,18-
334 trihydroxystearate, accumulated in the presence of Lmel) and cyclic nucleotides
335 (depleted in the presence of Lhel, Lmel and Lkul) (**Figure 6A and Supplementary**
336 **Figure 7**). Lhel was the only species depleting an ion corresponding to sugar alcohols
337 (mannitol, D-sorbitol, or L-glucitol) (**Figure 6A and Supplementary Figure 7**)
338 consistent with the specific upregulation of sugar alcohol PTS transporters in this species
339 (**Figure 4**).

340 Based on the untargeted metabolomics analysis, we conclude that the four species
341 target different metabolites, in particular secondary plant metabolites present in pollen.
342 In order to assess differences in the utilization of simple sugars and acids in more detail,
343 we analyzed the supernatants of cultures of the four strains after 0, 8, 16 and 24 h of
344 growth using GC-MS. We used a semi-targeted approach, where we identified a subset of

345 metabolites by preparing analytical standards and the others by using a reference library
346 (see methods). We identified 113 metabolites of which 46 showed a significant change in
347 abundance in at least one strain between timepoint 0h and 24h ($\log_2 FC \geq |2|$ and p-value
348 ≤ 0.01, Student's t-Test, BH correction) (**Supplementary Dataset 8**). All four species
349 showed mixed substrate utilization, i.e. they utilized several substrates simultaneously.
350 Moreover, most substrates were utilized by all four species, but often at different rates.
351 Many metabolites that we identified with the GC-MS had annotations comparable to the
352 ones found in the Q-TOF-based experiment. For example, we detected a compound
353 annotated as sugar alcohol, i.e. glucitol, that was consumed most efficiently by Lhel as
354 observed in the previous analysis (**Figure 6C**). Moreover, all four species consumed the
355 carboxylic acids citrate and malate (**Figure 6C** and **Supplementary Figure 8**), which
356 corresponded with the results of the Q-TOF-based experiment. Interestingly, Lkul and
357 Lhel consumed citrate at the fastest rate and they were also the two species that
358 upregulated gene clusters for citrate fermentation in the presence of pollen *in vivo* and *in*
359 *vitro* (**Figure 4**).

360 Lmel consumed several simple monosaccharides (such as glucose, fructose, allose
361 and mannose) at a slower rate than the other species, although having a similar growth
362 profile (**Figure 6C**, **Supplementary Figure 8** and **9**). This could indicate that Lmel has
363 specialized in the metabolism of pollen-derived glycosylated compounds (such as rutin,
364 **Figure 6B-C**) at the expense of fast consumption of generic substrates, which accords
365 with the upregulation of several gene clusters for the cleavage of such sugars from
366 polysaccharides or other glycosides (e.g. flavonoids) in presence of pollen (**Figure 4**).

367 In summary, our metabolomics results show that the four species specialize in the
368 utilization of different pollen-derived compounds, and that the observed metabolite

369 changes are to some extent consistent with the transcriptional changes observed in the

370 presence of pollen relative to the presence of simple sugars.

371

372 **Discussion**

373

374 Ecological processes governing the coexistence of microbes have been probed in
375 the laboratory using microbial communities of different complexity[12,14,29–33]. However,
376 few studies have examined the impact of the host on the coexistence of bacterial
377 symbionts of animals[14,32]. In particular, little is known about the extent to which closely
378 related species and strains can be stably maintained[8]. We capitalized on the experimental
379 tractability of honey bees and their gut microbiota and used a bottom-up approach to
380 study the coexistence of four closely related, naturally co-occurring *Lactobacillus* species.
381 We disentangled the effect of the diet and the host on the interactions between the four
382 species by serially passaging them through gnotobiotic bees or in culture tubes, under
383 two nutrient conditions (pollen versus simple sugars). Our results show that the
384 dynamics in the four-species community is governed by negative interactions, because
385 the growth of each member was lower in co-culture than in mono-culture, independent
386 of the environment (host or culture tube) and the nutrient condition (pollen or simple
387 sugars). This is consistent with previous observations that negative interactions
388 predominate in nutrient-rich environments[31,34–37]. Moreover, the four *Lactobacillus*
389 species harbor relatively small genomes (1.5-2Mb) with a conserved and streamlined
390 core metabolism and similar auxotrophies, suggesting overlapping nutritional
391 requirements[38–40].

392 The coexistence of bacterial symbionts can be facilitated by the host, e.g. by
393 providing a spatially structured environment that results in the physical separation of
394 competing strains[41–44], or by secreting metabolites that support niche specialization[45,46].
395 However, in the case of the four *Lactobacillus* species, such host-related features seem
396 not to be sufficient to support coexistence, because the four-species community was

397 rapidly dominated by a single species, when passaged through gnotobiotic bees that were
398 fed a simple sugar diet. In contrast, when providing a more diverse nutrition in the form
399 of pollen, we found that the four species were stably maintained both *in vivo* and *in vitro*.
400 We thus conclude that the coexistence of the four *Lactobacillus* species in the honey bee
401 gut primarily depends on the pollen diet of the host and not the host environment itself.

402 The challenges in replicating the native environment such that it is possible to
403 study relevant interactions of host-associated microbes *in vitro* are formidable. These
404 were highlighted in a recent study on the microbial community associated with the
405 freshwater polyp hydra that could not recapitulate the coexistence of the dominant
406 microbiota members *in vitro*[32]. Here, we aimed to approximate the nutritional conditions
407 in the honey bee gut by culturing the bacteria in pollen infused media, i.e. the natural diet
408 of bees. In both the *in vivo* and *in vitro* transfer experiment, we assessed the effect of
409 pollen on the dynamics of the community by comparing it to a simple sugar treatment.
410 Although not identical, the nutritional conditions *in vitro* were sufficiently similar as to
411 recapitulate the overall community dynamics observed *in vivo*: pollen nutrients
412 supported the stable coexistence of the four species, while the simple sugars led to the
413 dominance of a single species. As the bee and members of the bee gut microbiota pre-
414 digest pollen and sugars upstream of the rectum, it is difficult to exactly replicate the
415 metabolic environment of the rectum. For example, sucrose is largely absorbed via the
416 midgut epithelium and cleaved into glucose and fructose by host enzymes, while
417 fermentative bacteria such as *Gilliamella apicola* degrade and modify a diverse range of
418 carbohydrates in the ileum[25,47]. These metabolic alterations may explain some of the
419 differences observed between the *in vivo* and *in vitro* experiments, such as the dominance
420 of different species in the simple sugar conditions (sucrose and glucose respectively). We

421 therefore suspect that different species would dominate *in vitro* or *in vivo* with an
422 alternative simple sugar composition.

423 Our findings are consistent with the consumer-resource model, which predicts
424 that the number of species that can coexist depends on the number of available
425 resources[48]. Correspondingly, in the presence of a single substrate, such as in the case of
426 glucose *in vitro*, competition for the same nutrient results in the competitive exclusion of
427 all but one species. However, depending on the nutrient availability, the dietary transit
428 time, the crosstalk with the host, or the spatial structure of the gut, the ecological
429 processes governing bacterial coexistence may differ across host-associated
430 microbiomes. For example, the *Lactobacillus* species of the honey bee gut microbiota
431 primarily colonize the luminal space of the rectum, where partially digested pollen
432 accumulates. In contrast, some of the Proteobacteria of the bee gut microbiota adhere to
433 the epithelial surface of the ileum[49]. We expect that in the latter case interactions with
434 the host play a more important role for microbial coexistence than in the case of the
435 Lactobacilli in the rectum.

436 Although ecological interactions in bacterial communities have been investigated
437 across a wide range of experimental systems, few studies have tackled the molecular
438 mechanisms underlying coexistence. In some cases, cross-feeding of metabolic by-
439 products facilitates the maintenance of diversity in bacterial communities, such as after
440 passaging leaf and soil samples in single carbon sources[12]. However, cross-feeding does
441 not seem to play an important role in maintaining coexistence of the four *Lactobacillus*
442 species in this study. Unlike the above example, feeding a single carbon source led to the
443 extinction of all but one species. Our metabolomics analysis also did not reveal any major
444 metabolites that could potentially be cross-fed, i.e. were produced by one species and
445 utilized by another. Finally, we identified no transcriptional changes that would suggest

446 cross-feeding activities when comparing mono-cultures and co-cultures of the four
447 *Lactobacillus* species.

448 Instead, our combined transcriptomics and metabolomics analyses suggest that
449 coexistence is facilitated by specialization towards distinct pollen-derived nutrients. We
450 found that all four species upregulated carbohydrate transport and metabolism functions
451 dedicated to the utilization of different carbon sources in the presence of pollen when
452 colonizing the bee gut, and these changes were reproducible *in vitro*. Our metabolomics
453 analysis identified a number of pollen-derived glycosides that were utilized in a species-
454 specific manner. In particular, Lmel specialized in the utilization of flavonoids at the
455 expense of simple sugars, which may explain why this species rapidly went extinct in
456 presence of only simple sugars during the transfer experiments. While the importance of
457 pollen-derived flavonoids in niche partitioning needs to be validated, the species-specific
458 deglycosylation of these secondary plant compounds illustrates that the four species have
459 different hydrolytic capabilities that may also be involved in the cleavage of other
460 carbohydrates. The metabolic specialization on plant glycans may be a common
461 phenomenon in animal gut communities, as similar transcriptional changes have been
462 described in other gut symbionts when the host diet was supplemented with specific
463 plant glycans[50,51].

464 In contrast to the species specific metabolism of glycosides, we observed few
465 differences in the utilization of simple saccharides among the four species in our time-
466 resolved GC-MS analysis. While this may seem surprising, theoretical work has
467 established that resource preference for at least one substrate is sufficient to explain
468 coexistence[52]. Moreover, it is plausible that the four species utilize the same sugars, but
469 extract them from different pollen-derived glycans, such as starch, hemicellulose,
470 flavonoids, or other glycosylated secondary plant metabolites.

471 While this work focused on niche partitioning based on degradation of complex
472 carbohydrates, it is noteworthy that all four *Lactobacillus* species engaged to a variable
473 extent in co-fermentation of the carboxylic acids citrate and malate present in pollen. The
474 two species, Lkul and Lhel, that upregulated citrate fermentation pathways in the
475 presence of pollen also consumed citrate at the fastest rate. Citrate co-fermentation has
476 been linked to competitive advantages in lactic acid bacteria, though whether the varying
477 levels of co-fermentation contribute to colonization stability in this system remains an
478 outstanding question[53–55].

479 Previous work suggested that the large diversity of carbohydrate transport and
480 metabolism functions in the accessory gene pool of *Lactobacillus* Firm5 is an adaptation
481 to the pollen-based diet of the host and a consequence of the nutrient competition with
482 closely related species[22,38]. Our findings support this hypothesis and provide the first
483 experimental evidence for a link between the coexistence of the four *Lactobacillus*
484 species, the large diversity of carbohydrate metabolism functions in their genomes, and
485 the pollen diet of the host. Moreover, these results suggest that dietary differences
486 between host species or natural variation in pollen diversity influence the diversity of
487 *Lactobacillus* Firm5 and could, e.g., explain why the Asian honey bee, *Apis cerana,* harbors
488 only one species of this phylotype in its gut[56].

489 However, we have only tested a single strain of each of the four species. Therefore,
490 given the extensive genomic diversity within these species[22], more work is needed to
491 determine if the identified patterns of coexistence reflect stable ecological niches
492 occupied by the four species or are rather the result of the specific strains selected for
493 our experiments. In a recent study on pitcher plant microbiomes it was shown that even
494 strains that differ by only a few base pairs can have different ecological trajectories in
495 communities and coexist over extended period of time[8]. Expanding our approach to

strains within species presents an exciting next step to understand at which level discrete ecological niches are defined in the bee gut and how diversity can be maintained in such ecosystems.

500 # Materials and methods

501

Key Resources Table			
Reagent type (species) or resource	**Designation**	**Source or reference**	**Identifiers**
Strain, strain background (*Lactobacillus apis*)	Lapi	https://doi.org/10.1371/journal.pbio.2003467	Genome ID: 2684622912
Strain, strain background (*Lactobacillus helsingborgensis*)	Lhel	https://doi.org/10.1371/journal.pbio.2003467	Genome ID: 2684622914
Strain, strain background (*Lactobacillus melliventris*)	Lmel	https://doi.org/10.1371/journal.pbio.2003467	Genome ID: 2684622913
Strain, strain background (*Lactobacillus kullabergensis*)	Lkul	https://doi.org/10.1371/journal.pbio.2003467	Genome ID: 2684622911
Commercial assay or kit	QIAquick Gel Extraction Kit	Qiagen	#Cat 28706X4
Commercial assay or kit	Nucleospin RNA clean-up kit	Macherey-Nagel	#Cat 740903
Commercial assay or kit	Zymo-Seq RiboFree Total RNA Library kit	Zymo Research	#Cat R3000
Software, algorithm	R Studio software	R Studio (https://www.rstudio.com)	RRID:SCR_000432
Software, algorithm	Integrative Genomics Viewer	Integrative Genomics Viewer (https://software.broadinstitute.org/software/igv/)	RRID:SCR_011793

502

503 ## Culturing of bacterial strains

504 We used the following four bacterial strains of Lhel, Lmel, Lapi, and Lkul for our
505 experiments: ESL0183, ESL0184, ESL0185, and ESL0186 (Kešnerová et al., 2017). All
506 strains were precultured on solid De Man – Rogosa – Sharpe agar (MRSA) (supplemented
507 with 2% w/v fructose and 0.2% w/v L-cysteine-HCl) from glycerol stocks stored at -80˚C.
508 MRSA plates were incubated for three days in anaerobic conditions at 34˚C to obtain
509 single colonies. Single colonies were inoculated into a liquid carbohydrate-free MRS
510 medium (cfMRS[57]) supplemented with 4% glucose (w/v), 4% fructose (w/v) and 1% L-
511 cysteine-HCl (w/v) and incubated at 34˚C in anaerobic conditions without shaking.
512
513 ***In vivo* transfer experiments**
514 Bacterial colonization stocks were prepared from overnight cultures by washing
515 the bacteria in 1xPBS, diluting them to an OD_{600} = 1, and storing them in 25% glycerol at
516 -80˚C until further use. For colonization stocks containing all four species, cultures
517 adjusted to an OD_{600} = 1 were mixed at equal proportions. Microbiota-depleted bees were
518 obtained from colonies of *Apis mellifera carnica* located at the University of Lausanne
519 following the procedure described in Kešnerová et al. (2017). Colonization stocks were
520 diluted ten times in a 1:1 mixture of 1xPBS and sugar water (50% sucrose solution, w/v)
521 and 5 µL were fed to each bee using a pipette. Five days post-colonization, ten rectums
522 were dissected and homogenized in 1xPBS. An aliquot of each homogenized gut was used
523 for CFU plating to enumerate the total bacterial load and for amplicon sequencing to
524 obtain the relative abundance of each community member (see below). To serial passage
525 the community through microbiota-depleted bees, the ten homogenized gut samples
526 from the same treatment were pooled together and stored in 25% glycerol at -80˚C until
527 a new batch of microbiota-depleted bees was available. At the day of colonization, a
528 frozen aliquot of the pooled gut homogenate was thawed, diluted ten times in a 1:1

529 mixture of 1xPBS and sugar water (50% sucrose solution, w/v), and fed to newly
530 emerged microbiota-depleted bee as described above. This was repeated for a total of six
531 serial passages. Throughout the experiments all bees were kept on either a sugar water
532 or a sugar water/pollen diet according to the two dietary treatment. Food was provided
533 *ad libitum*.
534
535 ***In vitro* transfer experiment**
536 Each of the four strains was cultured in liquid medium overnight for about 16 h as
537 described above. The cultures were re-inoculated at an OD_{600} = 0.3 in fresh medium and
538 let grow for another 4 h at 34˚C with shaking (700 rpm). Bacterial cells were then washed
539 with 1xPBS, mixed in equal proportions, and inoculated at an OD_{600} = 0.05 in triplicates
540 in 96-deep well plates (SIGMA) containing cfMRS medium supplemented with either 2%
541 glucose (w/v), 10% pollen extract (v/v), or 10% pollen grains (v/v) in a final volume of
542 500 µL per well. Detailed information about pollen extract preparation can be found in
543 the Supporting methods section of Kešnerová et al. (2017). Pollen grain solutions were
544 prepared by adding 1.250 ml of ddH_2O to 80 mg of pollen grains crushed with the bottom
545 of a 15 mL falcon tube. The plates were incubated for 24 h at 34˚C under anaerobic
546 conditions without shaking (300 rpm). After 24 h of incubation, an aliquot of each sample
547 was subjected to CFU plating to enumerate the total bacterial load. Then, 1% of each
548 culture (i.e. 5 µL) was transferred to a plate with fresh medium supplemented with the
549 appropriate carbon sources and incubated again. These transfers were repeated 10,
550 respectively, 20 times for the two independent experiments. After each transfer, cultures
551 were washed once with 1xPBS and stored at -20˚C for amplicon sequencing analysis.
552 CFUs were counted after 24 h and at the final transfer.
553

554 **Amplicon sequencing**

555 The relative abundance of the four strains across all transfer experiments was
556 obtained using amplicon sequencing of a 199-bp long fragment of a housekeeping gene
557 encoding a DNA formamidopyrimidine-glycosylase which allows to discriminate the four
558 strains from each other[58].

559 For the *in vitro* transfer experiments, the PCR fragment was amplified from crude
560 cell lysates. They were generated by mixing 5 µL of culture with 50 µL of lysis solution,
561 containing 45 µL of lysis buffer (10 mM Tris- HCl, 1 mM EDTA, 0.1% Triton, pH 8), 2.5 µL
562 of lysozyme (20 mg/ml, Fluka) and 2.5 µL of Proteinase K solution (10 mg/ml, Roth). The
563 samples were incubated for 10 min at 37˚C, for 20 min at 55˚C, and for 10 min at 95˚C,
564 followed by a short spin before preparing the PCR (1 min, 1500 rpm). For the *in vivo*
565 transfer experiment, DNA was isolated from the homogenized gut samples using the hot
566 phenol protocol used in Kešnerová et al. (2017).

567 To amplify the gene fragment and to add the Illumina barcodes and adapters, the
568 two-step PCR strategy published in Ellegaard et al (2019) was used. For the first PCR, 5
569 µL of DNA or 5 µL of cell lysate were mixed with 12.5 µL of GoTaq Colorless Master Mix
570 (Promega), 1 µL of forward and reverse primer (5 µM, see **Supplementary Table 1**) and
571 5.5 µL of Nuclease-free Water (Promega). The PCR I was performed as follows: initial
572 denaturation (95˚C – 3 min), 30 times denaturation-annealing-extension (95˚C – 30 sec,
573 64˚C – 30 sec, 72˚C – 30 sec), final extension (72˚C – 5 min). To purify the amplicons, 15
574 µL of PCR product were mixed with 5 µL of a 5X Exo-SAP solution (15% Shrimp Alkaline
575 Phosphatase – 1000U/ ml – NEB, 10% Exonuclease I – 20000 U/ ml – NEB, 45% glycerol
576 80% and 30% dH2O). and incubated for 30 min at 37˚C and for 15 min at 80˚C. For the
577 second PCR reaction, 5 µL of purified PCR products were mixed with the same reagents
578 as before. The PCR program was the same as above with the exception that the annealing

579 temperature was set to 60˚C and the denaturation-annealing-extension steps were
580 repeated for only 8 times. The barcoded primers are listed in Supplementary Table 1. The
581 amplicons of the second PCR were purified using the Exo-SAP program as described
582 above.

583 To prepare the sequencing of the amplicons, DNA concentrations were measured
584 using Quant-iT™ PicoGreen® for dsDNA (Invitrogen). Each sample was adjusted to a DNA
585 concentration of 0.5 ng/µL and 5 µL of each sample were pooled together. The pooled
586 sample was loaded on a 0.9% agarose gel and gel-purified using the QIAquick Gel
587 Extraction Kit (Qiagen) following the manufacturer's instructions. The purified DNA was
588 prepared for sequencing following the Illumina MiniSeq System Guide for "denaturate
589 and dilute libraries" and then loaded on a Illumina MiniSeq Mid Output Reagent Cartridge
590 using the correspondent MiniSeq flow cell. Illumina reads were demultiplexed by
591 retrieving the unique barcodes of the different samples and quality-filtered using
592 Trimmomatic (Trimmomatic-0.35) (LEADING:28 TRAILING: 29 SLIDING WINDOW:4:15
593 MINLEN:90). Each forward and reverse read pair was assembled using PEAR (-m 290 -n
594 284 -j 4 -q 26 -v 10 -b 33)[59], and the assembled reads were assigned to the different
595 strains based on base pair positions with discriminatory SNP. See details in
596 Supplementary material.

597 To obtain absolute abundance data for each strain, we combined the relative
598 abundance data from the amplicon sequencing with CFU counts obtained from plating
599 homogenized bee guts in the case of the *in vivo* experiments (see above) or by carrying
600 out qPCR with *Lactobacillus* specific primers as described in Kešnerová et al. (2017) in
601 the case of the *in vitro* co-culture experiments (**Supplementary Table 1**,
602 **Supplementary Dataset 2**). For the *in vitro* transfer the stability of the four-species
603 community over time was calculated using the codyn R package[60].

604

605 **RNA extraction and sequencing**

606 For the *in vivo* RNA sequencing, microbiota-depleted bees were colonized with the
607 four species community as described above and fed with either sugar water and pollen
608 grains or with sugar water only. After 5 days of colonization, the rectums of five bees per
609 treatment (all kept in the same cage) were dissected and snap-frozen in liquid nitrogen
610 in separate tubes containing glass beads (0.1 mm dia. Zirconia/Silica beads; Carl Roth).
611 For RNA extraction, the tissue samples were suspended in 1 mL of TE buffer and
612 homogenized using a bead beater (45 m/s, 6 seconds). Then, 200 µL of an ice-cold STOP
613 solution (95% v/v ethanol, 5% v/v Aqua phenol (Roth)) was added to 1 ml of homogenate
614 and snap-frozen again in liquid nitrogen. Tubes were then thawed on ice and a previously
615 developed hot phenol RNA extraction protocol was followed[61]. For the *in vitro* RNA
616 sequencing, bacterial strains were cultured in triplicates in cfMRS supplemented with
617 either 1% w/v glucose or 1% w/v pollen extract. After 16 h of growth, 200 µL of STOP
618 solution was added to 1 mL of culture followed by the same steps as described above.

619 After the precipitation step, samples were treated with DNaseI (NEB) to degrade
620 DNA. RNA samples were purified using Nucleospin RNA clean-up kit (Macherey-Nagel)
621 following the manufacturer's instructions. RNA was eluted in RNase free-water and
622 stored at -80˚C until further use. RNA concentration and quality were assessed using
623 Nanodrop (ThermoFisher Scientific), Qubit (ThermoFisher Scientific, RNA – High
624 Sensitivity reagents and settings) and Bioanalyzer (Agilent). High-quality RNA samples
625 were selected to prepare RNA libraries. For the *in vivo* RNA sequencing, libraries were
626 prepared using the Zymo-Seq RiboFree Total RNA Library kit (Zymo Research). The
627 libraries were sequenced by the GTF facility of the University of Lausanne using HiSeq
628 4000 SR150 sequencing (150 bp reads) (Illumina). For the *in vitro* RNA sequencing,

629 libraries were prepared following the protocol developed by Avraham et al. [62]. Libraries
630 were then prepared for sequencing following the Illumina MiniSeq System guide for
631 denaturate and dilute libraries. Libraries were sequenced using the Illumina MiniSeq
632 technology using High Output Reagent Cartridges (150 bp reads) and MiniSeq flow cells.
633

634 **RNA sequencing analysis**

635 For the *in vitro* samples, raw reads were demultiplexed using a script provided by
636 Dr. Jelle Slager (Personal communication) For the *in vivo* samples, the reads were already
637 demultiplexed by the sequencing facility. For both experiments, the reads were trimmed
638 with Trimmomatic (Trimmomatic-0.35) (LEADING:30 TRAILING: 3 SLIDING
639 WINDOW:4:15 MINLEN:20). The quality of the reads was checked using FASTQC
640 (http://www.bioinformatics.babraham.ac.uk/projects/fastqc/). For the *in vivo* samples,
641 trimmed reads were sorted with sortmerna-4.2.0 to select only the non-rRNA reads for
642 the downstream analysis. Reads were mapped onto the genomes of the selected strains[63]
643 (Lapi, Lhel, Lmel and Lkul) using Bowtie (bowtie2-2.3.2). Gene annotations for the four
644 genomes were retrieved from IMG/mer[64]. Mapped reads were quality filtered for the
645 alignment length (CIGAR > 100 bp) and for the allowed mismatches in the sequence (NM
646 = 0-1). Quality filtered reads were then quantified using HTseq (Version 0.7.2).
647 Differential gene expression between samples cultured in pollen extract and samples
648 cultured in glucose, and between mono-cultures and co-cultures, was calculated using the
649 R package EdgeR[65]. Counts per million were calculated and only genes with at least 1
650 count per million were used for the analysis. EdgeR fits negative binomial models to the
651 data. The counts were normalized for RNA composition by adjusting the $\log_2$FC according
652 to the library size, and the quantile-adjusted conditional maximum likelihood (qCML)
653 method was used to estimate the common dispersion and the tag-wise dispersion.

654 Finally, the differential gene expression was determined using the exact test with a false
655 discovery rate (FDR) <5%. COG annotations were obtained from IMG/mer, and the
656 enrichment analysis for COG categories tested using the Fisher's exact test. Transcripts
657 per million (TPM) were visualized using the Integrated Genome Browser software[66].
658

659 **Untargeted metabolomics**

660 Metabolites were extracted from liquid cultures supplemented with 10% (w/v)
661 pollen extract at the inoculation time and after 16 h of incubation at 34˚C. For each liquid
662 culture sample, 300 µL was collected and centrifuged (20'000 g, 4˚C, 30 min), then 200
663 µL supernatant was transferred to a new tube and stored at -80˚C. After collection of all
664 samples, they were prepared for metabolomics analysis. The samples were thawed on ice
665 and centrifuged again (20'000 g, 4˚C, 5 min), then diluted 10 times with ddH_2O. For
666 metabolomics analysis, 25 µL of each diluted sample was sent in a 96-well plate on dry
667 ice to the laboratory of Prof. Uwe Sauer for analysis (ETH Zürich, Switzerland). Three
668 replicates of a pollen-extract dilution series (10 serial 2x dilutions) as well as undiluted
669 pollen-extracts and water used for performing the dilution series were included in the
670 metabolomics analysis. Because of the insolubility of flavonoid aglycones in a water
671 matrix, metabolites from liquid cultures supplemented with rutin were extracted using a
672 methanol-extraction protocol at the time of inoculation and after 16 h of growth by
673 adding 200 µL of methanol pre-cooled to -20˚C to 100 µL of culture. Tubes were vortexed
674 thoroughly and incubated for 5 min (4˚C, shaking 14'000 rpm). Samples where then
675 incubated at -20˚C for 1 h and centrifuged (20'000 g, 5 min). 200 µL of the supernatant
676 was transferred to a new tube and diluted 10 times in 70% methanol and 25 µL of each
677 diluted sample was sent to Zürich in Eppendorf tubes sealed with parafilm on dry ice. For
678 untargeted metabolomics analysis, each sample was injected twice (technical replicate)

679 into an Agilent 6550 time-of-flight mass spectrometer (ESI-iFunnel Q-TOF, Agilent
680 Technologies) as detailed in Kešnerová et al. (2017)[25]. In brief, m/z features (ions) were
681 annotated by matching their accurate mass-to-sum formulas of compounds in the KEGG
682 database accounting for deprotonation ($-H^+$). Alternative annotation can be found in
683 **Supplementary dataset 8.** When available, metabolites categories were assigned to ions
684 based on KEGG ontology.

685 Metabolomics data analysis was carried out using R version 3.6.3. Variation of raw
686 ion intensities obtained from untargeted metabolomics analysis for the two technical
687 replicates was determined by assessing the correlation between ion intensities of the
688 respective technical replicates. Then, mean ion intensities of technical replicates were
689 calculated. Time point comparisons (T = 0 h vs T = 16 h) were performed using t-tests
690 with Benjamini-Hochberg (BH) correction for multiple testing. $\log_2$FC values between the
691 two time-points were calculated with respect to the mean intensity in the T0 time point.
692 To identify pollen-derived ions, and distinguish them from background originating from
693 culture medium and experimental noise, the ion intensities of the pollen dilution series
694 were plotted for each ion and the R^2 of the obtained linear fit was extracted. In addition,
695 we calculated the $\log_2$FC difference between undiluted pollen and water. The R^2 values
696 were then plotted against the $\log_2$FC values, and stringent thresholds ($R_2 > 0.75$ and
697 $\log_2$FC > 2) were chosen to discriminate ions that are likely pollen-derived
698 (**Supplementary Figure 7**). All ions were included for downstream analysis (e.g. PCA)
699 and then they were discriminated between pollen-derived and non-pollen-derived.

700

701 **Semi-targeted Metabolomics via GC-MS**

702 Soluble metabolites were extracted from liquid cultures supplemented with 10%
703 pollen extract (w/v) at the inoculation time and after 8, 16 and 24 h of incubation. For

704 each liquid culture sample, 300 µL was collected and centrifuged (15'000 g, 4˚C, 15 min).
705 Then, 200 µL was transferred to a new tube, snap-frozen in liquid nitrogen, and stored at
706 -80˚C. Once that all the samples were collected, soluble metabolites were extracted. To
707 extract soluble metabolites, tubes were thawed on ice, and 75 µL of sample was combined
708 with 5 uL of 20 mM internal standard (norleucine and norvaline, (Sigma-Aldrich) and U-
709 $^{13}C_6$ glucose (Cambridge Isotope laboratories)). A volume of 825 µL of cold
710 methanol:water:chloroform (5:2:2) solution was added to the sample and vortexed for
711 30 sec. The tubes were incubated at -20°C for 90 min and vortexed 2x for 30 sec during
712 the incubation. Tubes were centrifuged for 5 min at 10'000g at 4°C. The supernatant was
713 removed and extraction was repeated using 400 µL of ice cold chloroform:methanol
714 (1:1), tubes were vortexed and left on ice for 30 min. Tubes were centrifuged 5 min at
715 8'000 rpm at 4°C and the liquid phase was transferred to the previous extracted aqueous
716 phase. 200 µL of water was added and tubes were centrifuged 5 min at 8000 rpm. The
717 aqueous phase was transferred to a 2 mL microcentrifuge tube. The aqueous extract was
718 dried using a vacuum concentrator at ambient temperature overnight (Univapo 150 ECH
719 vacuum concentrator centrifuge). Once dried, the samples were dissolved in 50 µL of 20
720 mg/ml methoxyamine hydrochloride in pyridine for 1.5 h at 33°C followed by
721 derivatization with N-Methyl-N-(trymethylsolyl)trifluoroacetamide (MSTFA, Sigma
722 Aldrich) for 2 h at 35°C.

723 Aliquots (1 µL) were injected on an Agilent 8890/5977B GC-MSD. The samples
724 were injected in split mode (20:1) with an inlet temperature of 250 °C. The VF-5ms (30
725 m x 250 µm x 0.25 µm) column was held initially at 125 °C for 2 mins, ramped at 5 °C / min
726 to 250 °C, ramped at 15 °C to 300 °C, and held for 5 min. The MS was run in full scan mode
727 (50-500 m/z) at a speed of 5 Hz. Peaks from the total ion chromatogram (TIC) were
728 identified by matching retention times and spectra to an in-house library that was built

729 by comparing selected T=0h and T=24h samples against the NIST library, as well as our
730 library of analytical standards. Compounds are noted as either confirmed with our own
731 standards, or the best match and associated matching factor against the NIST library are
732 reported (**Supplementary Dataset 8**). Peaks were picked and integrated using the
733 Agilent MassHunter Quantitative Analysis software. Peak areas were normalized to the
734 internal standards. The data were processed using R version 3.6.3 and mean intensities
735 and $\log_2$FC between time-points were calculated as described above for the untargeted
736 metabolomics analysis.
737

738 **Analysis-code and data availability**

739 The complete custom code for all the analyses is available on GitHub:
740 (https://github.com/silviabrochet). The amplicon sequencing data and the RNA
741 sequencing data are available under the NCBI Bioproject PRJNA700984 and the GEO
742 record GSE166724. All differential expression analysis results of this study are included
743 in **Supplementary Dataset 9**.
744

Acknowledgments

We thank Kirsten Ellegaard for the critical reading of the manuscript and discussions on the experimental design. We also thank Sara Mitri for providing feedback on the manuscript. We are grateful to Simon Maréchal for his help with the transfer experiments. This project was funded by the ERC-StG "MicroBeeOme" (grant 714804), the Swiss National Science Foundation (grant 31003A_160345 and 31003A_179487), the Human Frontier Science Program Young Investigator (grant RGY0077/2016) and the NCCR Microbiomes.

Competing interests

The authors declare that they have no competing interests.

758 **References**

759

760 1. Ley, R. E. *et al.* Evolution of mammals and their gut microbes. *Science (80-.).* **320**,
761 1647–1651 (2008).
762 2. Dethlefsen, L., McFall-Ngai, M. & Relman, D. A. An ecological and evolutionary
763 perspective on humang-microbe mutualism and disease. *Nature* **449**, 811–818
764 (2007).
765 3. Elton, C. Competition and the Structure of Ecological Communities. *J. Anim. Ecol.*
766 **15**, 54–68 (2016).
767 4. Ley, R. E., Peterson, D. A. & Gordon, J. I. Ecological and evolutionary forces shaping
768 microbial diversity in the human intestine. *Cell* **124**, 837–848 (2006).
769 5. Foster, K. R., Schluter, J., Coyte, K. Z. & Rakoff-Nahoum, S. The evolution of the host
770 microbiome as an ecosystem on a leash. *Nature* **548**, 43–51 (2017).
771 6. Koskella, B. & Brockhurst, M. A. Bacteria-phage coevolution as a driver of
772 ecological and evolutionary processes in microbial communities. *FEMS Microbiol.*
773 *Rev.* **38**, 916–931 (2014).
774 7. Chesson, P. Mechanisms of Maintainance of Species Diversity. *Annu. Rev. Ecol.*
775 *Syst.* **31**, 343–66 (2000).
776 8. Leonora S. Bittleston, Matti Gralka, Gabriel E. Leventhal, Itzhak Mizrahi, O. X. C.
777 Context-dependent dynamics lead to the assembly of functionally distinct pitcher-
778 plant microbiomes. *Nat Commun* **3**, 1–31 (2019).
779 9. Berasategui, A. *et al.* Gut microbiota of the pine weevil degrades conifer
780 diterpenes and increases insect fitness. *Mol. Ecol.* **26**, 4099–4110 (2017).
781 10. Martens, E. C., Chiang, H. C. & Gordon, J. I. Mucosal Glycan Foraging Enhances
782 Fitness and Transmission of a Saccharolytic Human Gut Bacterial Symbiont. *Cell*
783 *Host Microbe* **4**, 447–457 (2008).
784 11. Madi, N., Vos, M., Murall, C. L., Legendre, P. & Shapiro, B. J. Does diversity beget
785 diversity in microbiomes? *bioRxiv* 1–26 (2020). doi:10.1101/612739
786 12. Goldford, J. E. *et al.* Emergent simplicity in microbial community assembly.
787 *Science (80-.).* **361**, 469–474 (2018).
788 13. Rakoff-Nahoum, S., Foster, K. R. & Comstock, L. E. The evolution of cooperation
789 within the gut microbiota. *Nature* **533**, 255–259 (2016).
790 14. Lopez, A. O., Vega, N. M. & Gore, J. Interspecies bacterial competition determines

791 community assembly in the C. elegans intestine. *ISME J.* (2021).
792 doi:10.1101/535633
793 15. Venturelli, O. S. *et al.* Deciphering microbial interactions in synthetic human gut
794 microbiome communities. *Mol. Syst. Biol.* **14**, 1–19 (2018).
795 16. Li, L. *et al.* An in vitro model maintaining taxon-specific functional activities of the
796 gut microbiome. *Nat. Commun.* **10**, (2019).
797 17. Jalili-Firoozinezhad, S. *et al.* A complex human gut microbiome cultured in an
798 anaerobic intestine-on-a-chip. *Nat. Biomed. Eng.* **3**, 520–531 (2019).
799 18. Nikolaev, M. *et al.* Homeostatic mini-intestines through scaffold-guided organoid
800 morphogenesis. *Nature* **585**, 574–578 (2020).
801 19. Martinson, V. G. *et al.* A simple and distinctive microbiota associated with honey
802 bees and bumble bees. *Mol. Ecol.* **20**, 619–628 (2011).
803 20. Kwong, W. K. & Moran, N. A. Gut microbial communities of social bees. *Nat. Rev.*
804 *Microbiol.* **14**, 374–384 (2016).
805 21. Ellegaard, K. M. & Engel, P. Beyond 16S rRNA community profiling: Intra-species
806 diversity in the gut microbiota. *Front. Microbiol.* **7**, 1–16 (2016).
807 22. Ellegaard, K. M., Engel, P. Genomic diversity landscape of the honey bee gut
808 microbiota. *Nat. Commun.* **10.1**, 1–13 (2019).
809 23. Engel, P., Martinson, V. G. & Moran, N. a. Functional diversity within the simple gut
810 microbiota of the honey bee. *Proc. Natl. Acad. Sci. U. S. A.* **109**, 11002–11007
811 (2012).
812 24. Ellegaard, K. M. *et al.* Extensive intra-phylotype diversity in lactobacilli and
813 bifidobacteria from the honeybee gut. *BMC Genomics* **16**, 1–22 (2015).
814 25. Kešnerová, L., Mars, R. A. T., Ellegaard, K. M., Sauer, U. & Engel, P. Disentangling
815 metabolic functions of bacteria in the honey bee gut. *PLoS Biol.* 1–28 (2017).
816 26. Kešnerová, L. *et al.* Gut microbiota structure differs between honeybees in winter
817 and summer. *ISME J.* **14**, 801–814 (2020).
818 27. Fuhrer, T., Heer, D., Begemann, B. & Zamboni, N. High-throughput, accurate mass
819 metabolome profiling of cellular extracts by flow injection-time-of-flight mass
820 spectrometry. *Anal. Chem.* **83**, 7074–7080 (2011).
821 28. Beekwilder, J. *et al.* Characterization of Rhamnosidases from Lactobacillus
822 plantarum and Lactobacillus acidophilus. *Appl. Environ. Microbiol.* **75**, 3447–3454
823 (2009).

824 29. Wright, Erik S., and K. H. V. Inhibitory interactions promote frequent bistability
825 among competing bacteria. *Nat Commun* **7**, 11274 (2016).
826 30. Friedman, J., Higgins, L. M. & Gore, J. Community structure follows simple
827 assembly rules in microbial microcosms. *Nat. Ecol. Evol.* **1**, 1–7 (2017).
828 31. Piccardi, P., Vessman, B. & Mitri, S. Toxicity drives facilitation between 4 bacterial
829 species. *Proc. Natl. Acad. Sci. U. S. A.* **116**, 15979–15984 (2019).
830 32. Deines, P., Hammerschmidt, K. & Bosch, T. C. G. Microbial species coexistence
831 depends on the host environment. *MBio* **11**, 1–13 (2020).
832 33. Logan M. Higgins, J. F. H. S. & J. G. Co-occurring soil bacteria exhibit a robust
833 competitive hierarchy and lack of non-transitive interactions. *bioRxiv* 1–16
834 (2017).
835 34. Foster, K. R. & Bell, T. Competition, not cooperation, dominates interactions
836 among culturable microbial species. *Curr. Biol.* **22**, 1845–1850 (2012).
837 35. Berry, D. & Widder, S. Deciphering microbial interactions and detecting keystone
838 species with co-occurrence networks. *Front. Microbiol.* **5**, 1–14 (2014).
839 36. Coyte, K. Z., Schluter, J. & Foster, K. R. The ecology of the microbiome: Networks,
840 competition, and stability. *Science (80-.).* **350**, 663–666 (2015).
841 37. Ghoul, M. & Mitri, S. The Ecology and Evolution of Microbial Competition. *Trends*
842 *Microbiol.* **24**, 833–845 (2016).
843 38. Ellegaard, K., Brochet, S., Emery, O., Glover, N. & Hadadi, N. Genomic changes
844 underlying host specialization in the bee gut symbiont Lactobacillus Firm5. *Mol.*
845 *Ecol.* **28**, 2224–2237 (2019).
846 39. Ellegaard, K. M. *et al.* Extensive intra-phylotype diversity in lactobacilli and
847 bifidobacteria from the honeybee gut. *BMC Genomics* **16**, 1–22 (2015).
848 40. Kwong, W. K. & Moran, N. A. Gut microbial communities of social bees. *Nat. Rev.*
849 *Microbiol.* **14**, 374–384 (2016).
850 41. Gude, S. *et al.* Bacterial coexistence driven by motility and spatial competition.
851 *Nature* **578**, 588–592 (2020).
852 42. Kim, H. J., Boedicker, J. Q., Choi, J. W. & Ismagilov, R. F. Defined spatial structure
853 stabilizes a synthetic multispecies bacterial community. *PNAS* **105**, 18188–18193
854 (2008).
855 43. Mitri, S., Clarke, E. & Foster, K. R. Resource limitation drives spatial organization
856 in microbial groups. *ISME J.* **10**, 1471–1482 (2016).

857 44. Hallatschek, O., Hersen, P., Ramanathan, S. & Nelson, D. R. Genetic drift at
858 expanding frontiers promotes gene segregation. *Proc. Natl. Acad. Sci. U. S. A.* **104**,
859 19926–19930 (2007).
860 45. Schluter, J. & Foster, K. R. The Evolution of Mutualism in Gut Microbiota Via Host
861 Epithelial Selection. *PLoS Biol.* **10**, (2012).
862 46. McLoughlin, K., Schluter, J., Rakoff-Nahoum, S., Smith, A. L. & Foster, K. R. Host
863 Selection of Microbiota via Differential Adhesion. *Cell Host Microbe* **19**, 550–559
864 (2016).
865 47. Crailsheim, K. Intestinal transport of sugars in the honeybee (Apis mellifera L.). *J.*
866 *Insect Physiol.* **34**, 839–845 (1988).
867 48. Tilman, D. A consumer-resource approach to community structure. *Integr. Comp.*
868 *Biol.* **26**, 5–22 (1986).
869 49. Zheng, H., Steele, M. I., Leonard, S. P., Motta, E. V. S. & Moran, N. A. Honey bees as
870 models for gut microbiota research. *Lab Anim. (NY).* **47**, 317–325 (2018).
871 50. Sonnenburg, J. L. *et al.* Glycan foraging in vivo by an intestine-adapted bacterial
872 symbiont. *Science (80-.).* **307**, 1955–1959 (2005).
873 51. Zheng, H. *et al.* Division of labor in honey bee gut microbiota for plant
874 polysaccharide digestion. *Proc. Natl. Acad. Sci. U. S. A.* **116**, 25909–25916 (2019).
875 52. Meszéna, G., Gyllenberg, M., Pásztor, L. & Metz, J. A. J. Competitive exclusion and
876 limiting similarity: A unified theory. *Theor. Popul. Biol.* **69**, 68–87 (2006).
877 53. Laëtitia, G., Pascal, D. & Yann, D. The Citrate Metabolism in Homo- and
878 Heterofermentative LAB: A Selective Means of Becoming Dominant over Other
879 Microorganisms in Complex Ecosystems. *Food Nutr. Sci.* **05**, 953–969 (2014).
880 54. Magni, C., De Mendoza, D., Konings, W. N. & Lolkema, J. S. Mechanism of citrate
881 metabolism in Lactococcus lactis: Resistance against lactate toxicity at low pH. *J.*
882 *Bacteriol.* **181**, 1451–1457 (1999).
883 55. Jimeno, J., Lazaro, M. J. & Sollberger, H. Antagonistic interactions between
884 propionic acid bacteria and non-starter lactic acid bacteria. *Lait* **75**, 401–413
885 (1995).
886 56. Ellegaard, K. M., Suenami, S., Miyazaki, R. & Engel, P. Vast Differences in Strain-
887 Level Diversity in the Gut Microbiota of Two Closely Related Honey Bee Species.
888 *Curr. Biol.* **30**, 2520-2531.e7 (2020).
889 57. Donnell, M. M. O., Forde, B. M., Neville, B., Ross, P. R. & Toole, P. W. O.

890 Carbohydrate catabolic flexibility in the mammalian intestinal commensal
891 Lactobacillus ruminis revealed by fermentation studies aligned to genome
892 annotations. *Microb. Cell Fact.* **10**, 1–11 (2011).
893 58. Ellegaard, K. M. *et al.* Genomic changes underlying host specialization in the bee
894 gut symbiont Lactobacillus Firm5. *Mol. Ecol.* **28**, 2224–2237 (2019).
895 59. Zhang, J., Kobert, K., Flouri, T. & Stamatakis, A. PEAR: A fast and accurate Illumina
896 Paired-End reAd mergeR. *Bioinformatics* **30**, 614–620 (2014).
897 60. Hallett L, Avolio M, Carroll I, Jones S, MacDonald A, Flynn D, Slaughter P,
898 Ripplinger J, Collins S, Gries C, J. M. (2020). codyn: Community Dynamics Metrics.
899 doi: 10.5063/F1N877Z6, R package version 2.0.5,
900 https://github.com/NCEAS/codynHallett L, Avoli,
901 https://github.com/NCEAS/codyn.
902 61. Sharma, C. M. *et al.* The primary transcriptome of the major human pathogen
903 Helicobacter pylori. *Nature* **464**, 250–255 (2010).
904 62. Avraham, R. *et al.* A highly multiplexed and sensitive RNA-seq protocol for
905 simultaneous analysis of host and pathogen transcriptomes. *Nat. Protoc.* **11**,
906 1477–1491 (2016).
907 63. Ellegaard, K. M. & Engel, P. New Reference Genome Sequences for 17 Bacterial
908 Strains of. *Microbiol. Resour. Announc.* **7**, 4–6 (2018).
909 64. Chen, I. M. A. *et al.* The IMG/M data management and analysis system v.6.0: New
910 tools and advanced capabilities. *Nucleic Acids Res.* **49**, D751–D763 (2021).
911 65. Robinson, M. D., McCarthy, D. J. & Smyth, G. K. edgeR: A Bioconductor package for
912 differential expression analysis of digital gene expression data. *Bioinformatics* **26**,
913 139–140 (2009).
914 66. Nowlan H. Freese, David C. Norris, and A. E. L. Integrated Genome Browser:
915 Visual analytics platform for genomics. *Bioinformatics* (2016).

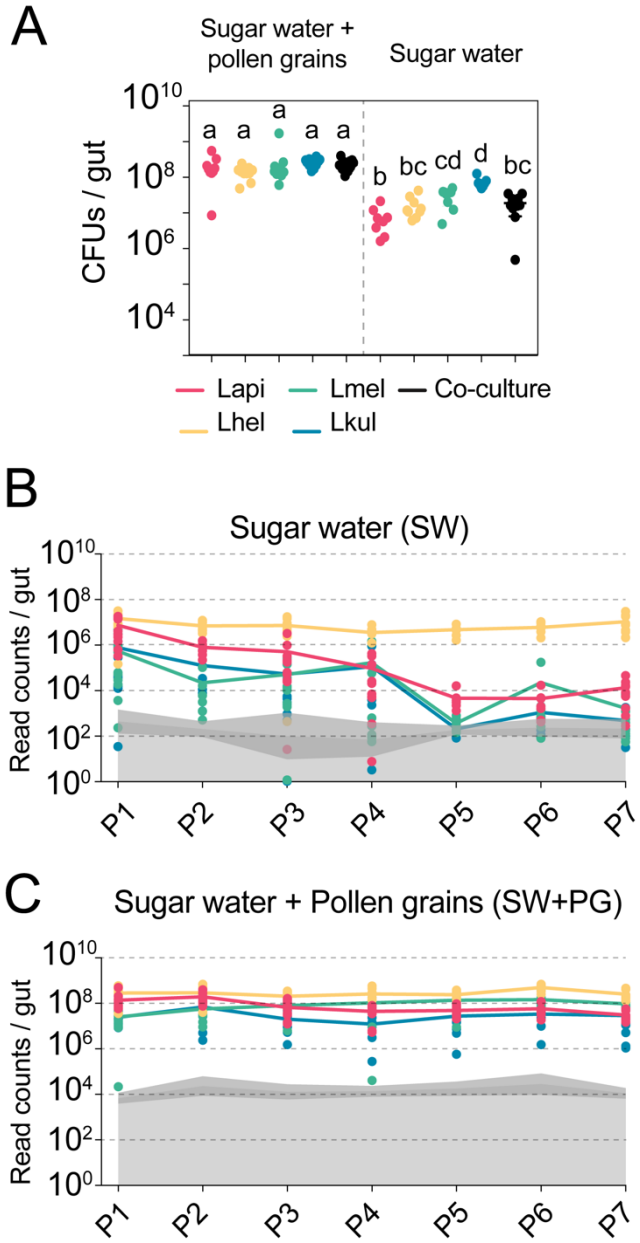

Figure 1. The presence of dietary pollen facilitates the stable coexistence of the four *Lactobacillus* species in the honey bee gut. (A) Bacterial abundance (CFUs) in the gut of gnotobiotic bees (n= 7-10) colonized with the four species separately or together under two different dietary conditions. Bees were sampled five days after colonization. Statistical differences (ANOVA with Tuckey post-hoc test and BH correction) are depicted by different letters. **(B, C)** Changes in the absolute abundance of each member of the four-species community across the seven serial passages (P1-P7) through the gut of gnotobiotic bees. The absolute abundance of each species was determined by multiplying the total number of CFUs with the relative abundance of each species in the community. Grey areas represent the limit of detection which can vary depending on the sequencing depth of each replicate (see methods). Therefore, the average limit of detection and the 95% confidence intervals are shown.

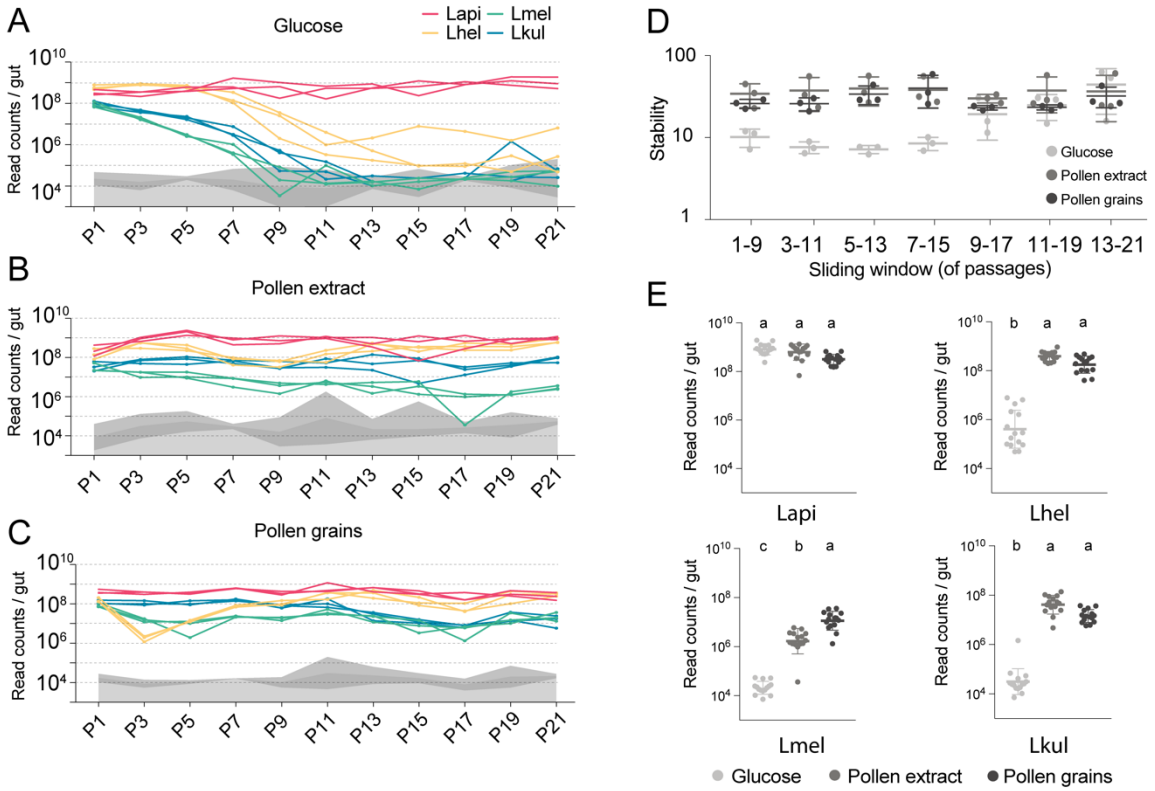

Figure 2. The stable coexistence of the four *Lactobacillus* species can be recapitulated *in vitro* in the presence of pollen. (A-C) Changes in total abundance of the four species when serial passaged in co-culture for 21 times in minimal medium supplemented with **(A)** 2% (w/v) glucose, **(B)** 10% (v/v) pollen extract**,** and **(C)** 10% (v/v) pollen grains**.** The absolute abundance of each species was determined by multiplying the total number of CFUs with the proportion of each strain in a given sample as based on amplicon sequencing (see methods). Grey areas indicate the limit of detection as explained in the methods. **(D)** Community stability of each replicate calculated based on the species abundances for a sliding window of five passages with a step size of 1. **(E)** Absolute abundance of each species across the three treatments considering the replicates of passages 13-21, which is when the community reached stability. Statistical differences (ANOVA with Tuckey post-hoc test and BH correction) are depicted by different letters.

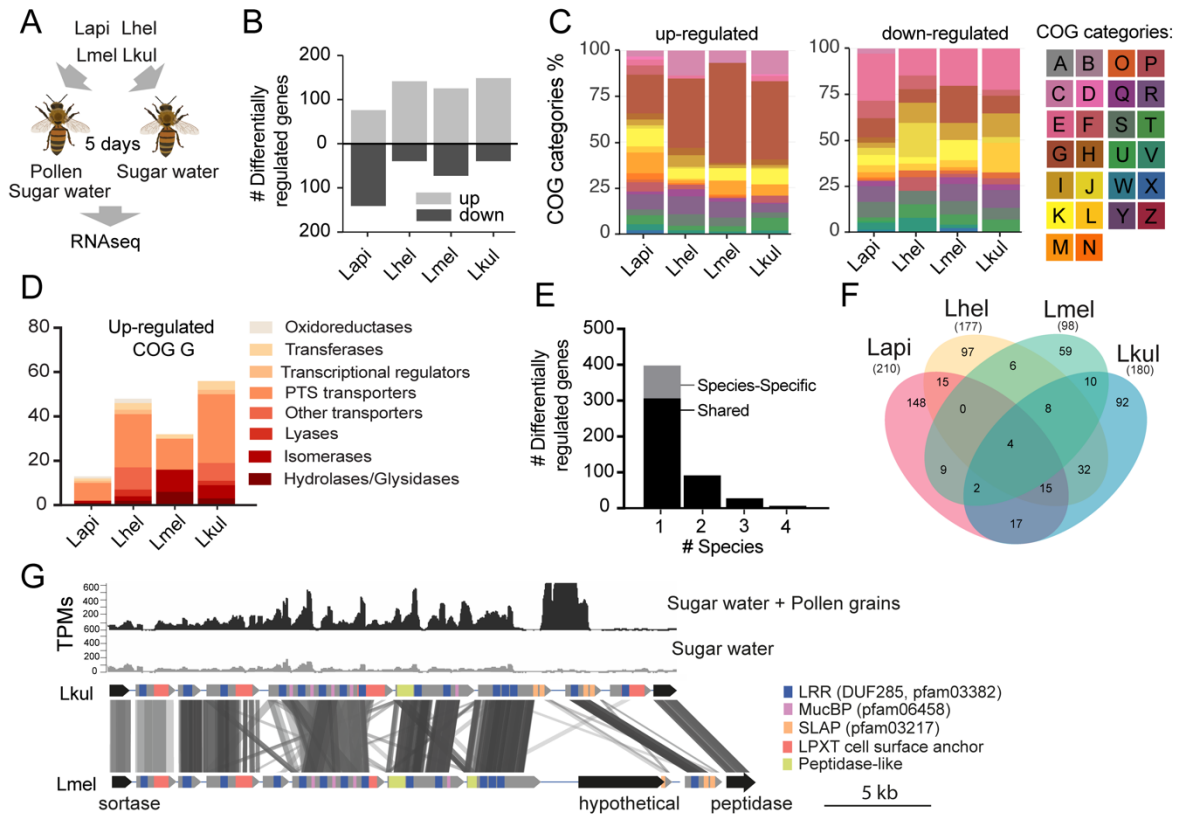

Figure 3: Transcriptome analysis of the four *Lactobacillus* species during co-colonization of gnotobiotic bees. **(A)** Schematic outline of the RNA-Seq experiment. **(B)** Number of differentially regulated genes ($\log_2 FC \geq |2|$ and p-value ≤ 0.01) in each species during co-colonization of gnotobiotic bees fed either pollen and sugar water (PG+SW) or sugar water only (SW). Up- and down-regulated genes are shown in different grey tones. **(C)** COG categories of genes up- or down-regulated by the four species in SW+PG if compared to SW. For COG definitions, see Supplementary Table 2 **(D)** Functional sub-categories of COG 'G' genes upregulated in SW+PG if compared to SW. **(E)** Barplot displaying numbers of gene families differentially regulated in one species, two species, three species, or four species. Gene families differentially regulated in only one species are split into those that have homologs in the other species or that are species-specific.**(F)** Venn diagram showing overlap of gene families (based on gene homology) differentially regulated in the four species. **(G)** Transcripts per million (TPM) for two representative samples of the SW+PG and the SW treatments over a genomic region of Lkul encoding *Lactobacillus*-specific surface proteins. The genomic region of Lkul is compared to a similar region identified in Lmel which is also differentially regulated across the two treatments (expression profile not shown). Similarity between genes is shown by vertical lines. Grey tones indicate level of similarity. Surface protein-encoding genes are show in grey with the different domains and motifs shown according to the color legend.

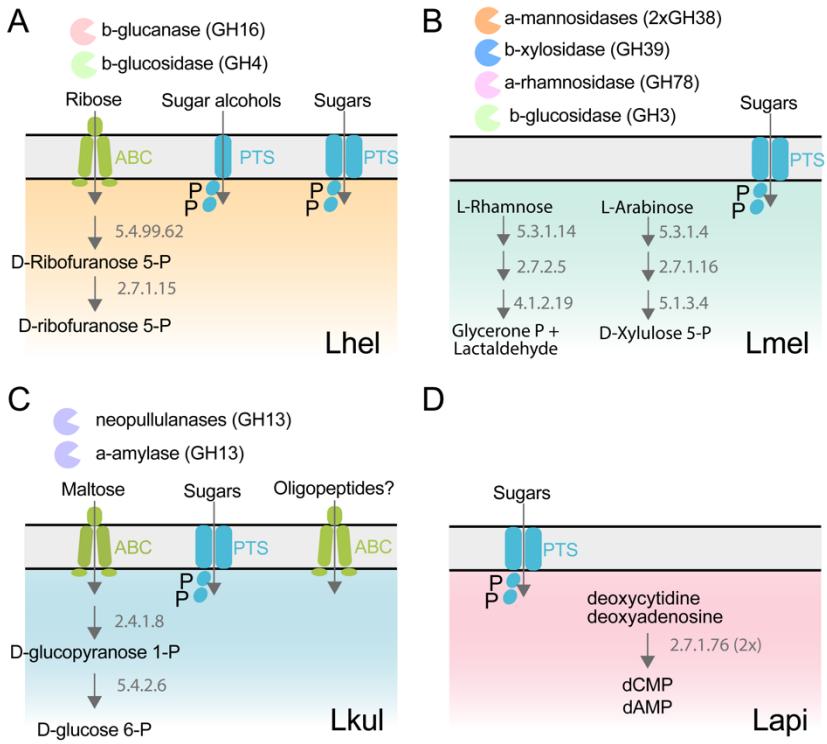

954

955 **Figure 4. The four *Lactobacillus* species upregulate different carbohydrate metabolism functions during gut**
956 **colonization of gnotobiotic bees. (A)** Lhel, **(B)** Lmel, **(C)** Lkul, **(D)** Lapi. Only enzymes and transporters that are
957 upregulated in a species-specific manner in the pollen treatment versus the sugar water treatment are shown. The
958 figure is not exhaustive, but highlights the main differences that could be identified based on gene annotations among
959 all differentially regulated genes (**Supplementary Dataset 4**). Glycosidases belonging to different CAZyme families are
960 represented by different colors. ABC: ABC transporters, PTS: phosphotransferase system transporters. Numbers
961 indicate EC numbers of upregulated enzymatic steps.

962

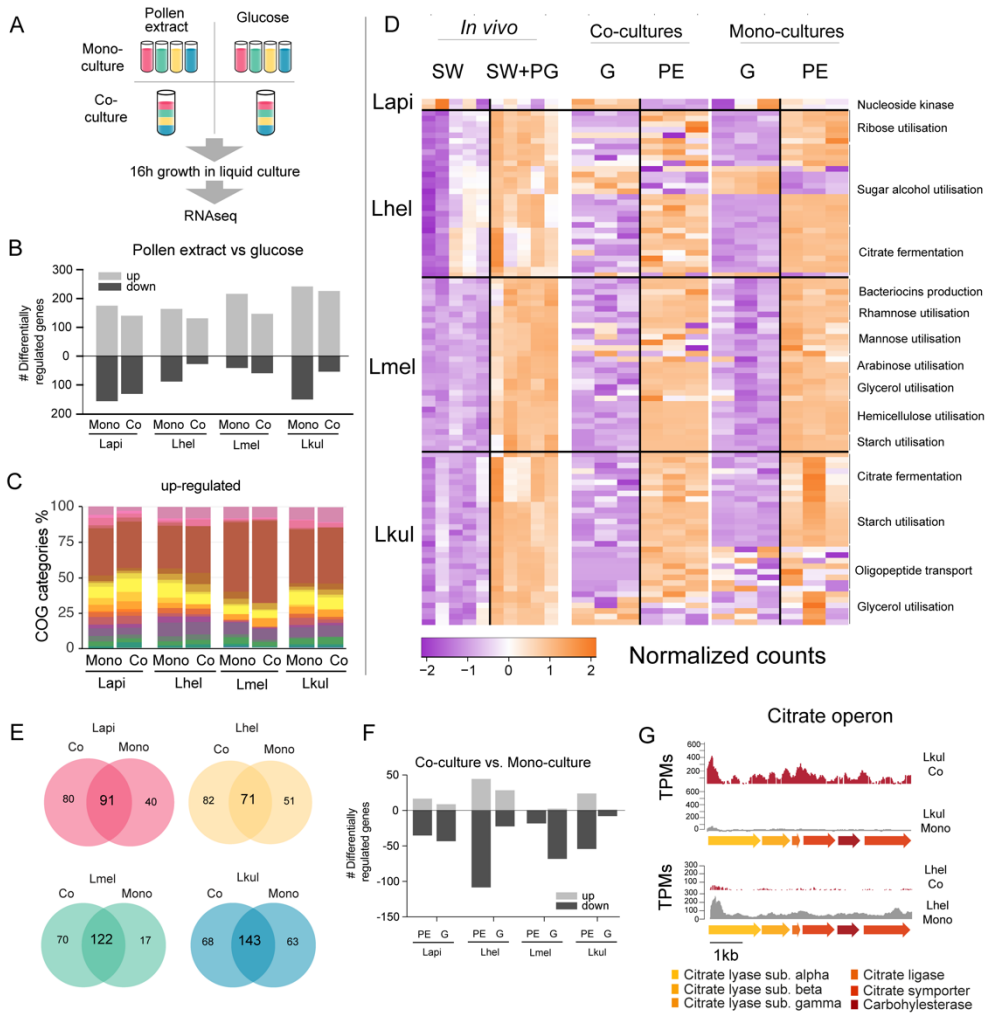

Figure 5: Transcriptome analysis of the four *Lactobacillus* species grown *in vitro* in pollen extract or in glucose. **(A)** Scheme of the 2x2 experimental design. Species were grown alone or together, in either glucose (G) or pollen extract (PE). **(B)** Number of differentially regulated genes in each of the four species in the presence of PE if compared to G. Mono, mono-culture, Co, co-culture. Up- and down-regulated genes are shown in different gray tones. **(C)** COG categories of genes up-regulated by the four species in the presence of PE if compared to G. The colors are the same as in Figure 3C. For COG definitions, see Supplementary Table 2. **D)** Heatmap displaying normalized counts of selected genes differentially regulated across the *in vivo* and *in vitro* RNA-Seq experiments. We selected metabolic genes and gene clusters that were identified in the in vivo experiment to be differentially regulated across the two treatments and which could be assigned a putative function based on annotation. Counts were normalized for each gene and dataset separately, i.e. *in vivo*, co-cultures, and mono-cultures. **(E)** Venn diagrams displaying the overlap of the genes differentially regulated between the PE and G treatment when the four species were grown in co-culture (Co) and mono-culture (Mono). **(F)** Number of differentially regulated genes in each of the four species in co-culture relative to mono-culture. Up- and down-regulated genes are shown in different gray tones. **(G)** Transcripts per million (TPM) over a genomic region of Lkul and Lmel encoding genes for citrate fermentation (i.e. citrate operon) for a representative sample of the co-culture and the mono-culture treatment when grown in PE.

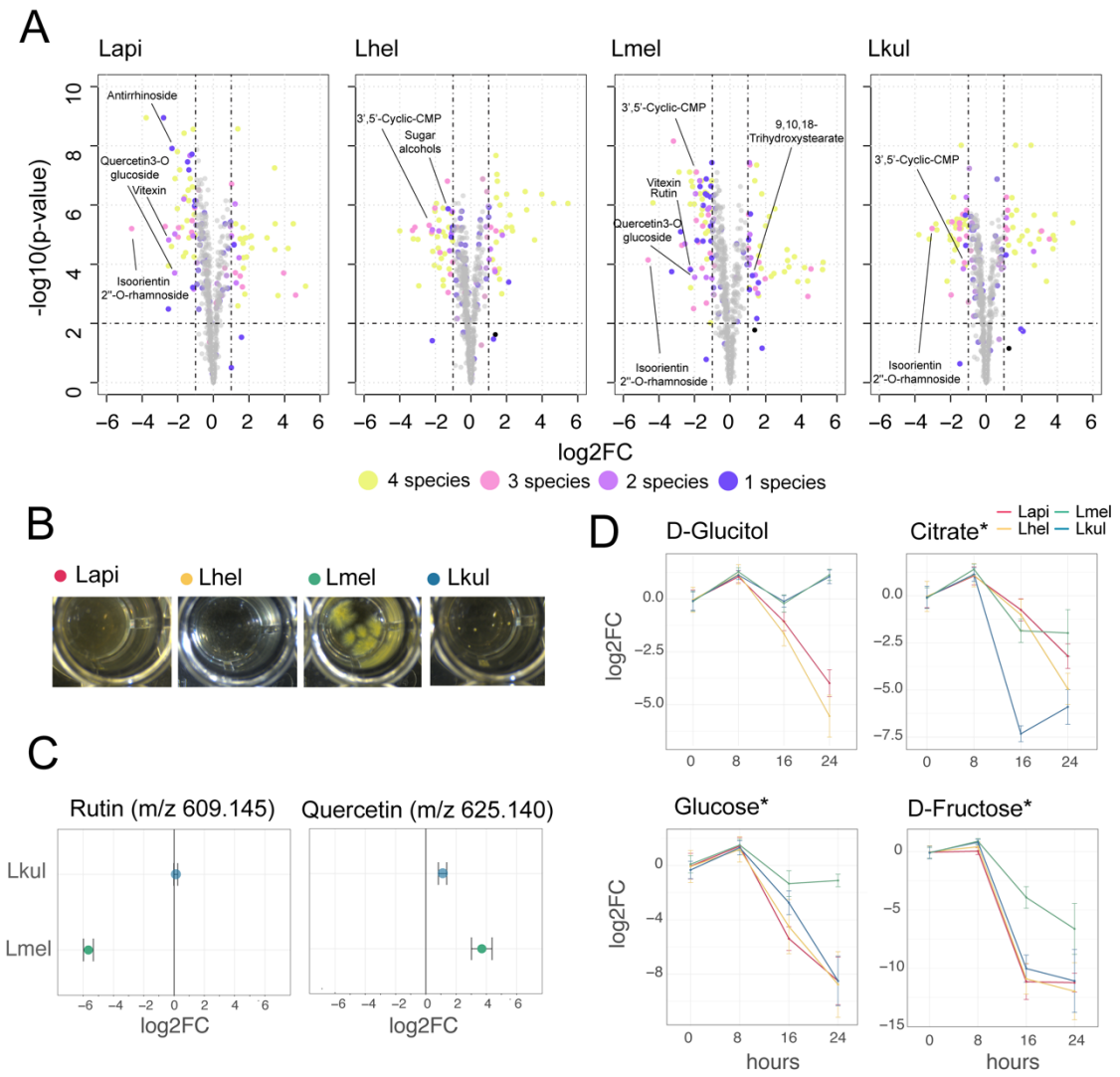

Figure 6. Metabolomics analysis shows differences in the utilization of pollen-derived glycosides across the four *Lactobacillus* species. (A) Volcano plots displaying ions with significant fold changes (FC) for each of the four species after 16 h of growth in pollen extract versus glucose. Each dot corresponds to an ion in the untargeted metabolomics dataset. Different colors represent ions that significantly change over time in one, two, three, or four species. Dashed black lines represent the significance thresholds: p-value < 0.01 and log2FC < -1 or > 1. **(B)** Culture wells of the four species grown in cfMRS + 0.05% rutin after 16 h of incubation. The yellow precipitate is only visible for Lmel. **(C)** Rutin and quercetin detection in spent medium of Lmel and Lkul grown in cfMRS + 0.05% rutin after 16 h of incubation (n=5). **(D)** Changes in key metabolites during growth measured by GC-MS (n=5). Log_2FC relative to time point 0 is plotted. Time is reported in hours. * Indicates metabolites whose identity was confirmed using analytical standards. For m/z values see **Supplementary Dataset 8**.